

# Squaric Ester-Based Nanogels Induce No Distinct Protein Corona but Entrap Plasma Proteins into their Porous Hydrogel Network

Anne Huppertsberg, Christian Leps, Irina Alberg, Christine Rosenauer, Svenja Morsbach, Katharina Landfester, Stefan Tenzer, Rudolf Zentel, and Lutz Nuhn\*

After intravenous administration of nanocarriers, plasma proteins may rapidly adsorb onto their surfaces. This process hampers the prediction of the nanocarriers' pharmacokinetics as it determines their physiological identity in a complex biological environment. Toward clinical translation it is therefore an essential prerequisite to investigate the nanocarriers' interaction with plasma proteins. Here, this work evaluates a highly "PEGylated" squaric ester-based nanogel with inherent prolonged blood circulation properties. After incubation with human blood plasma, the nanogels are isolated by asymmetrical flow-field flow fractionation. Multiangle light scattering measurements confirm the absence of significant size increases as well as aggregation upon plasma incubation. However, proteomic analyses by gel electrophoresis find minor absolute amounts of proteins (3 wt%), whereas label-free liquid chromatography mass spectrometry identify 65 enriched proteins. Interestingly, the relative abundance of these proteins is almost similar to their proportion in pure native plasma. Due to the nanogels' hydrated and porous network morphology, it is concluded that the detected proteins rather result from passive diffusion into the nanogel network than from specific interactions at the plasma particle interface. Consequently, these results do not indicate a classical surface protein corona but rather reflect the highly outer and inner stealth-like behavior of the porous hydrogel network.

However, effective nanocarrier application often requires intravenous injection,<sup>[1,2]</sup> which makes the characterization of the nanocarrier's plasma protein affinity commonly referred to as protein corona essential for their clinical translation. After injection into the complex protein-rich medium, blood proteins may rapidly adsorb onto the nanocarrier's surface. As a result, the nanocarrier's surface properties may be altered to such an extent that its pharmacokinetics become hard to predict. This emphasizes that the protein corona constitutes a major aspect of the nanocarriers' physiological identity.<sup>[3-5]</sup> In particular, the nanocarriers' biodistribution and cell uptake may change, which can further impair passive or active targeting strategies. Protein corona formation is typically specific for each nanocarrier as it is determined by the carrier's composition, surface property, and morphology.<sup>[2]</sup> Various factors may be involved in protein adsorption process, however, its main driving forces can be attributed to hydrophobic and electrostatic interactions.<sup>[6]</sup> These attractive forces recruit plasma proteins to the

particle plasma interface in order to minimize surface tension and stabilize the particle by the formation of protein coronas. Within different nanocarrier systems (e.g., colloids, polymeric micelles, nanogels) these interactions can vary greatly as they also depend on their different internal morphologies, and thus

## 1. Introduction

Physio-chemical properties of nanocarriers can easily be analyzed during their shelf-life under aqueous buffer conditions, yet, in complex physiological media this is no longer possible.

A. Huppertsberg, C. Rosenauer, S. Morsbach, K. Landfester, L. Nuhn  
 Max Planck Institute for Polymer Research  
 55128 Mainz, Germany  
 E-mail: lutz.nuhn@mpip-mainz.mpg.de

C. Leps, S. Tenzer  
 Institute for Immunology  
 University Medical Center of Mainz  
 55131 Mainz, Germany

I. Alberg, R. Zentel  
 Department of Chemistry  
 Johannes Gutenberg University Mainz  
 55128 Mainz, Germany

L. Nuhn  
 Chair of Macromolecular Chemistry  
 Faculty of Chemistry and Pharmacy  
 Julius Maximilian University Würzburg  
 97074 Würzburg, Germany

 The ORCID identification number(s) for the author(s) of this article can be found under <https://doi.org/10.1002/marc.202200318>

© 2022 The Authors. Macromolecular Rapid Communications published by Wiley-VCH GmbH. This is an open access article under the terms of the Creative Commons Attribution-NonCommercial License, which permits use, distribution and reproduction in any medium, provided the original work is properly cited and is not used for commercial purposes.

DOI: 10.1002/marc.202200318

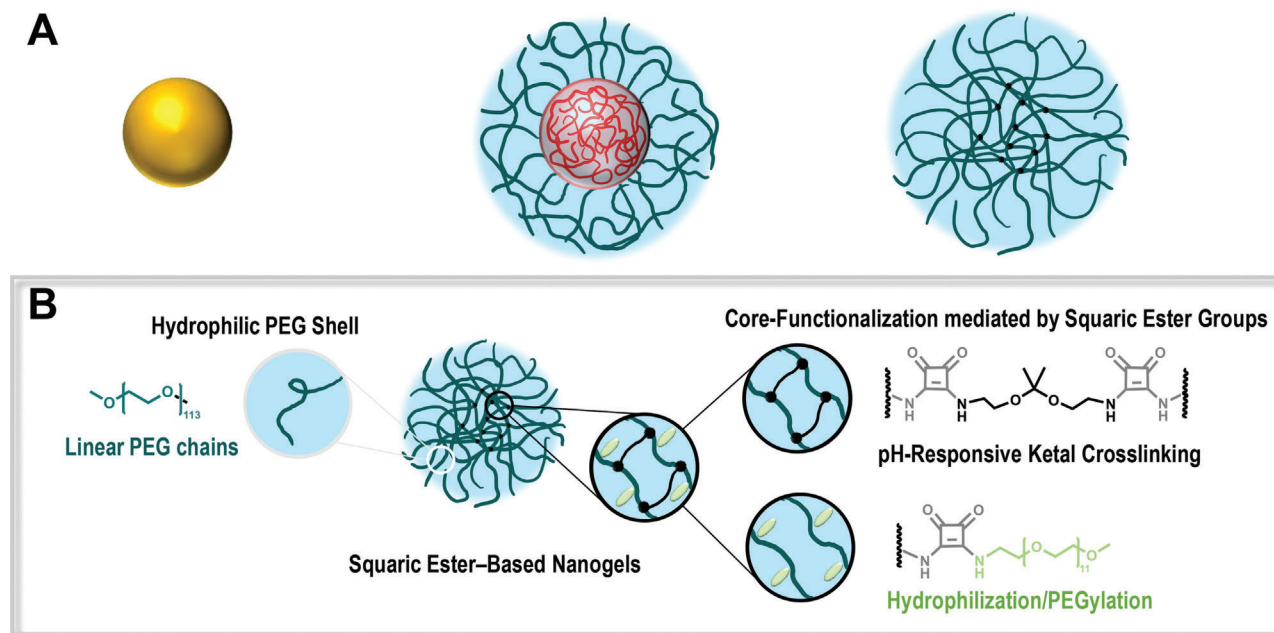


**Figure 1.** A) Scheme of common nanocarrier systems such as colloidal nanoparticles (left), polymeric micelles (middle), and polymeric nanogels (right). In contrast to colloids, micelles and nanogels have no sharp surface, but possess a hydrated shell, which consists of swollen polymer chains. While polymeric micelles have a hard, dense core due to its hydrophobic nature, nanogels are mostly hydrophilic and water-swollen systems. B) Chemical composition of squaric ester-based nanogels: Their hydrophilic shell comprises linear PEG chains, while squaric amide groups in their core mediate its functionalization through pH-responsive crosslinking as well as hydrophilization with short PEG chains. The covalent crosslinks in the nanogel's core generate a network structure that becomes fully hydrophilic due to the conjugation of additional short PEG chains. Thus, the nanogels structure can be described as nano-sized water-swollen polymer network.

also the corresponding interfaces they provide.<sup>[7]</sup> Consequently, it must be investigated for every individual nanocarrier system, whether it forms a classical surface protein corona or not.

In this work, we investigated whether squaric ester-based nanogels would provide such a distinct protein corona. The nanogels are derived from amphiphilic block copolymers consisting of a linear hydrophilic poly(ethylene glycol) (PEG) chain as well as a poly(methacrylamide) block with pendant squaric ester amides. After self-assembly, their amine-reactive cores are sequentially converted by pH-responsive ketal crosslinkers, dyes, and oligo(ethylene glycols) affording fully hydrophilic nanogels (D-NG) as recently described in detail.<sup>[8,9]</sup> Interestingly, in previous works a long blood circulation of the nanocarriers after intravenous injection was observed: Even after 72 h, intact nanogels (and some disassembled single polymer chains) could be found circulating in the blood stream of mice by fluorescent correlation spectroscopy (FCS) measurements of full blood samples from mice.<sup>[10]</sup> During these measurements, we also did not observe any significant interaction with the blood plasma components under the applied FCS measurement conditions.

In this study, we decided to further explore the correlation between their profound stability in the blood stream and their potential protein corona formation using asymmetrical flow-field flow fractionation (AF4) combined with label-free liquid chromatography mass spectrometry (LC-MS). LC-MS as protein corona characterization method was recently introduced to elucidate the protein corona of several nano-sized drug carriers.<sup>[3,11,12]</sup> The AF4 technique allows for separation by size, but in contrast to conventional size chromatography, shear forces are reduced

to a minimum. Due to the resulting very mild separation conditions, AF4 has shown to be the ideal technique to facilitate the separation of low-density nanocarriers including their “hard” or even “soft” protein corona.<sup>[13,14]</sup>

While so far mainly the protein corona of colloidal particles,<sup>[15–17]</sup> that are easily isolated by centrifugation, had been studied, Alberg et al. investigated first non-colloidal polymer nanocarriers by means of their established AF4 LC-MS method.<sup>[12,18]</sup> Due to the low density of these non-colloidal polymeric nanocarriers, which is comparable to plasma/water, their isolation by centrifugation would not have been feasible. The studied nanocarriers were either polymeric brushes or crosslinked polymeric micelles consisting of a dense hydrophobic core, whose surface is coated and intrinsically stabilized by fully hydrated, hydrophilic “stealth” polymers according to the Whitesides’ rules.<sup>[19]</sup> Due to steric repulsion by the adsorbed water molecules in the nanocarriers shell, a direct contact of the proteins with the hydrophobic core is—in case of a perfect coating—prevented. In contrast to these systems, our squaric ester-based nanogels are fully hydrophilic systems, since not only their shell comprises the hydrophilic stealth material PEG, but also their core is largely “PEGylated” (Figure 1A). The morphology of these completely swollen nanogels may be described as network of polymer chains, which are interconnected in the core by covalent crosslinks (Figure 1B).<sup>[7]</sup> Based on this “porosity,” the nanogel’s structure may be comparable with a sponge allowing diffusion of proteins into the polymer network (depth of diffusion depends on mesh size). Due to the described morphology, the nanogel’s potential to form a protein corona

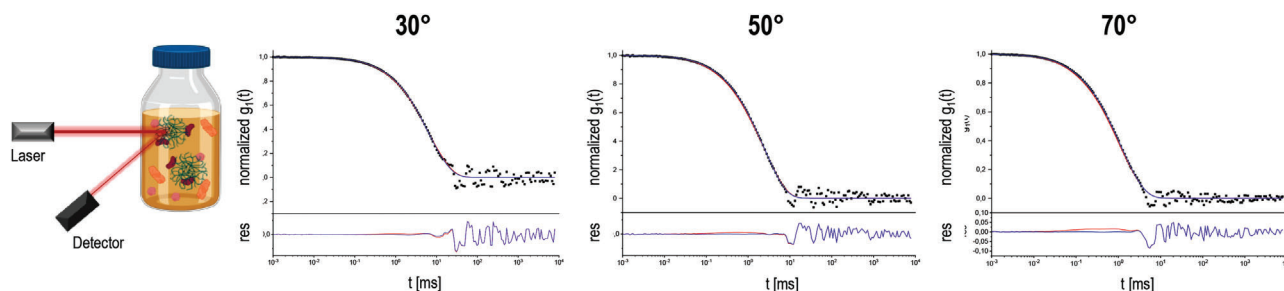


**Figure 2.** Multiangle DLS study of pH-responsive squaric ester-based nanogels (D-NG) after incubation with full human blood plasma. The graphs show autocorrelation functions  $g_1(t)$  (black dots) of the NG/plasma mixture at scattering angles of 30°, 50°, or 70°. The fit of the sum of the individual components is displayed by the red line, whereas the dark blue line represents the fit including an additional aggregation function. Lower graphs display the residuals which result from the difference between data and the two fits.

may differ from the nanocarriers with impermeable hydrophobic cores and dense hydrophilic surfaces previously examined by Alberg et al. for which a negligible protein adsorption (less than one protein per nanocarrier) was found.<sup>[12]</sup> And most of all, the nanogels differ drastically from nanocarriers with hard, sharp surfaces<sup>[15–17]</sup> where proteins can only access the interface and get easily adsorbed by hydrophobic and electrostatic interactions in order to minimize surface tension.

Nonetheless, protein corona formation has not per se negative consequences. Not only nanocarriers without protein corona but also systems with pronounced corona can have long blood circulation and serve their purpose. However, when the protein adsorption is a prerequisite for the nanocarrier's *in vivo* fate, this may cause issues since the protein corona formation is expected to strongly depend on the individual patient.<sup>[20,21]</sup> Thus, nanocarriers without protein corona are usually more favorable, as their *in vivo* behavior may be more predictable since their inherent properties would allow longer plasma stability and blood circulation to fulfill their delivery purposes.

## 2. Results and Discussion

In this study, we investigated the protein affinity of pH-responsive squaric ester-based nanogels (D-NG) after plasma incubation and subsequent AF4 isolation. As the nanocarriers have shown a high blood stability in previous studies,<sup>[8,10]</sup> we wanted to take a further look at the correlation between their profound stability and potential protein corona formation by these methods. First, the nanogel's behavior in full human blood plasma was analyzed by multiangle dynamic light scattering (DLS) applying a strategy by Rausch et al.<sup>[22]</sup> which allows for determining particle aggregation in plasma. Measurements were recorded after 1 h incubation time at 37 °C (Figure 2). As shown earlier, 1 h of incubation is usually a sufficient time for the formation of a protein corona,<sup>[3]</sup> and follows previous protocols by Alberg and co-workers<sup>[12,18]</sup> who further investigated the potential formation of a protein corona for other non-colloidal polymeric nanocarriers. The black dots in the upper graphs show the autocorrelation function of the nanogel/plasma mixture at scattering angles of 30°, 50°, or 70°, while the fit of the sum of the individual components is represented by the red line, and the blue line displays the fit including an additional aggregation function if required. In the lower graphs the residuals resulting from the difference between these two fits are shown. The absence of deviations be-

tween both lines indicates that no aggregation occurred and the nanogel's size remained similar upon plasma incubation. This characteristic was further supported by previous FCS measurements after plasma incubation up to 24 h at 37 °C, in which the unaltered autocorrelation functions implied that neither aggregation nor degradation of the nanocarrier took place under these physiologically relevant conditions.<sup>[8]</sup>

Next, D-NG was again incubated in human blood plasma for 1 h at 37 °C, but now the previously described AF4 method by Alberg<sup>[12]</sup> was applied to separate the squaric ester-based nanogels including potentially adsorbed proteins from the plasma protein mixture. For this purpose, AF4 has shown to be the ideal technique, since it allows the separation of nanocarrier systems with densities similar to plasma including only softly adsorbed proteins. Methods like centrifugation could not facilitate separations of these low-density nanogels.

The nanogel/protein incubation mixture was injected into the AF4 device (Figure 3A). The retention of the various sample compartments in the AF4 channel was determined by the applied crossflow (0.75 mL min<sup>-1</sup>), which was optimized beforehand according to the nanocarrier's size and ensured an adequate separation of the nanogel and potential nanogel-protein complexes from free plasma proteins.

The AF4 elugrams with recordings either by a UV-vis or a light scattering detector are depicted in Figure 3B. The first peak in both elugrams can be identified by means of the plasma control (red) as free protein peak. As most plasma proteins have a size between 6 to 10 nm,<sup>[22]</sup> they elute faster than the markedly larger NGs.<sup>[23,24]</sup> The second peak corresponds to D-NG as deduced by comparison of the D-NG control (D-NG incubated in PBS, green) with the plasma incubated D-NG (blue). No shift of the nanocarrier peak to later elution times was evident after plasma incubation, which excludes a size increase due to significant plasma aggregation. Thus, these observations confirm again that the nanocarrier neither aggregates nor forms a significantly large protein corona on its surface. Additionally, no intensity increase of the rinse peak (third peak) at the end of the measurement was found. Since this peak is characteristic of large sample compartments such as nanocarrier aggregates (or lipoproteins), which elute only after the crossflow is stopped, this further supports that no D-NG/protein aggregates were formed upon plasma incubation.

Interestingly, we observed a slight intensity increase for the D-NG peak in the AF4 elugrams. We hypothesized that this

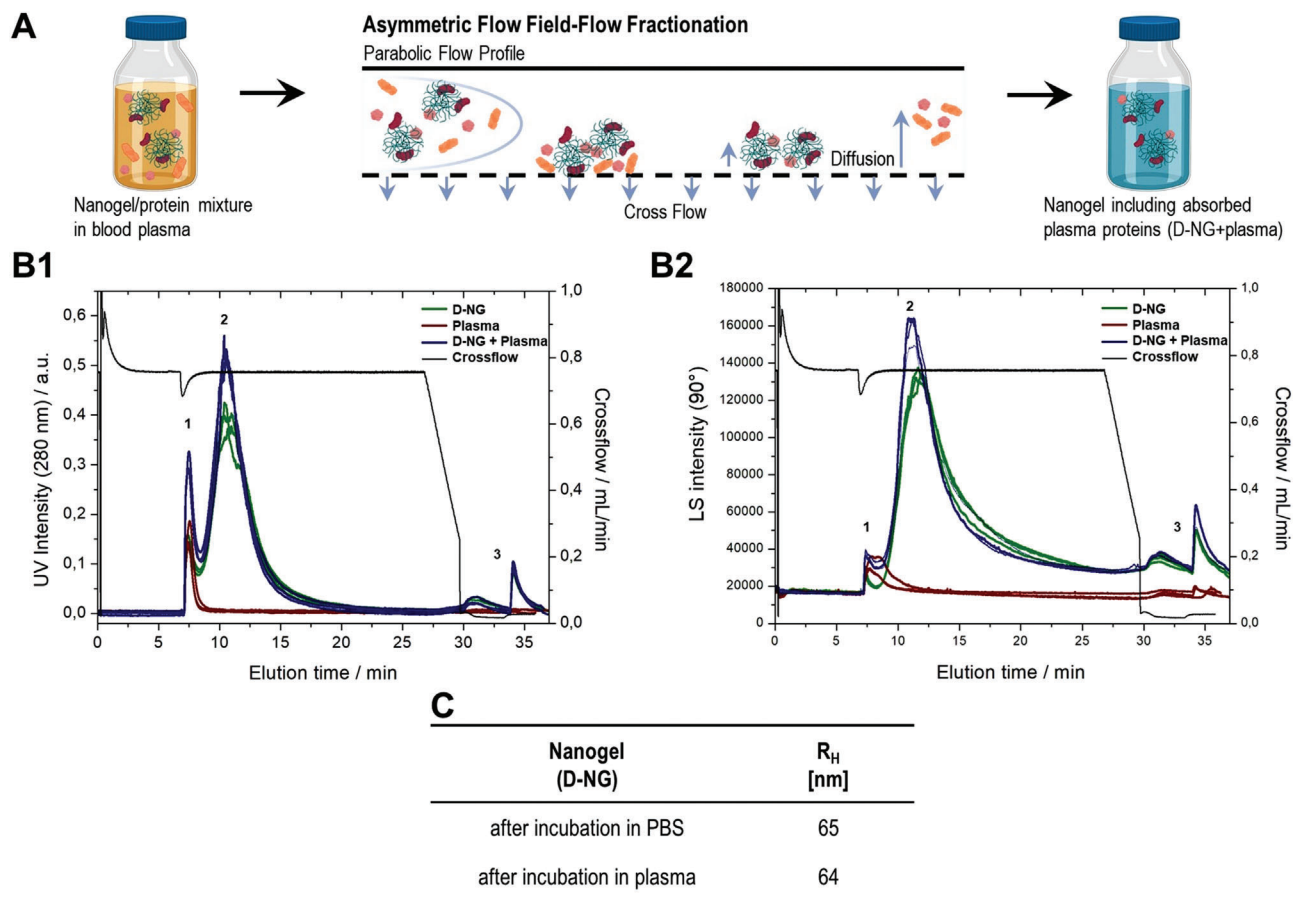


**Figure 3.** A) Scheme of asymmetric field-flow fractionation (AF4) separating nanogels after plasma incubation from unbound proteins. AF4 elugrams of D-NG sensed by B1) UV detector at 280 nm and B2) LS intensity at 90°. D-NG incubated in PBS (green), D-NG incubated in plasma (blue), plasma only (red) as well as applied crossflow (black). All experiments were performed in triplicates. C) Hydrodynamic radius ( $R_H$ ) of D-NG after incubation in different mediums and subsequent AF4 fractionation.

increase could refer to a minimal incorporation of proteins inside the swollen nanogel network, which could not get released under the applied separation conditions but remains rather marginal as it does not affect the nanocarrier's size.

For additional characterization, the D-NG elution area between 10 and 17 min was isolated for all three samples. Multi-angle DLS measurements of the isolated nanocarriers fractions further attested that the hydrodynamic radius ( $R_H$ ) of D-NG remained identical upon plasma incubation (Figure 3C and Figure S1, Supporting Information) and thus, further promoted the fact that no significant interactions of plasma proteins and nanocarriers obviously occurred which would lead to a size increase. We speculate that the nanogel's high degree of "PEGylation" (in their shell as well as inside their core) provides sufficient stealth properties in plasma or full blood. The observed profound stability also corresponds to previous findings showing their low uptake by phagocytosing cells and long-lasting circulation in the blood stream after intravenous injections.<sup>[8,10]</sup>

Despite the absence of a size increase for our squaric ester-based nanogel, the inclusion of small amounts of plasma proteins in the D-NG could not be fully excluded. For the characterization of these proteins, we performed SDS PAGE analysis. In Figure 4B a silver-stained SDS PAGE gel of the three iso-

lated AF4-fractions during D-NG elution time (D-NG incubated in PBS, D-NG incubated in plasma, and plasma only) as well as decreasing amounts of human serum albumin (HSA, 170, 17, 1.7 ng) is shown. For the plasma incubated D-NG (pocket 3) a distinct band between 50 and 60 kDa was evident. As HSA, the most abundant protein in human plasma, was applied to the gel as reference (pocket 5–7), this band could be assigned to the latter.

To ascertain whether HSA is a true corona component, comparison with the AF4 co-eluting plasma and D-NG control is mandatory. Since no band for the D-NG incubated in PBS (pocket 2) as well as for the pure plasma fraction (pocket 4) was evident, two factors could be excluded: On the one hand, the observed band could not be caused by protein impurities during nanocarrier fabrication and, on the other hand, HSA was not simply co-eluting as free protein. Thus, HSA appears to be somehow interacting with D-NG and therefore co-eluting during AF4 separation.

However, the absolute amount of HSA is obviously relatively low. Only the very sensitive silver staining with a detection limit in the low ng-range<sup>[25]</sup> was able to detect the band, while the less sensitive Coomassie staining (low  $\mu$ g-range detection limit)<sup>[26]</sup> did not reveal any band for the D-NG incubated in plasma (Figure S2, Supporting Information). To determine the absolute

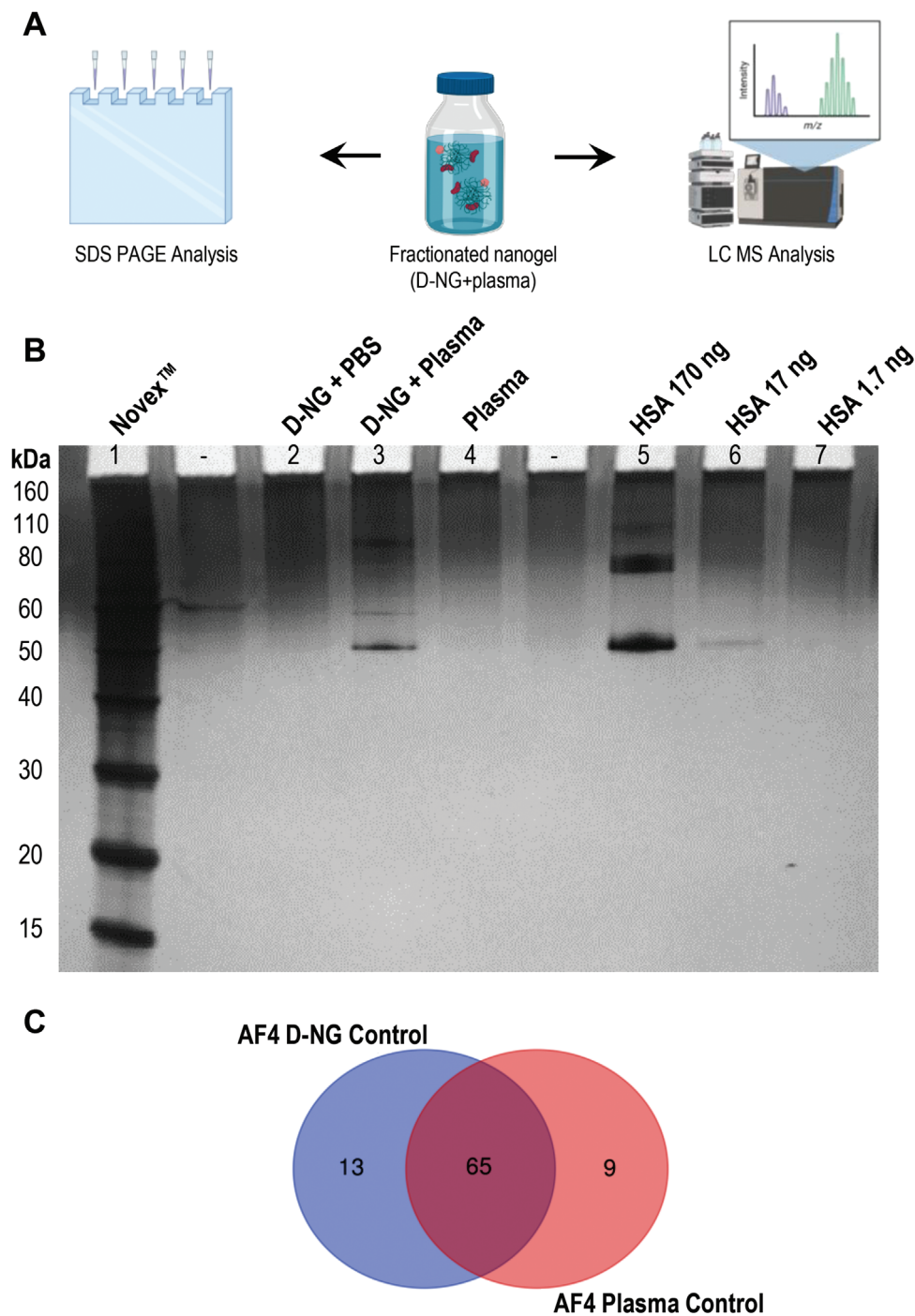


**Figure 4.** A) Scheme of protein characterization of AF4 isolated D-NG fraction by SDS PAGE and LC-MS. B) Silver-stained SDS PAGE gel of D-NG after AF4 purification. 1) Novex Sharp Pre-Stained Protein Standard, 2) D-NG incubated in PBS, 3) D-NG incubated in plasma, 4) Plasma collected during D-NG elution time, 5) HSA 170 ng, 6) HSA 17 ng, 7) HSA 1.7 ng. C) Proteomic LC-MS analysis of D-NG incubated in plasma as well as D-NG and plasma control. The Venn diagram indicates the number of identified proteins (overlap area) significantly enriched on D-NG incubated in plasma compared to the plasma and D-NG controls.

amount of HSA, various quantities of pure HSA (pocket 5–7) were used for a comparative analysis of their silver-stained band intensities with the band intensity originating from the D-NG incubated in plasma sample. Via a calibration by the applied HSA samples, the HSA band of the D-NG sample was quantified and

calculated to correspond to a total amount of 52 ng (for more details on the data analysis, see Figure S3, Supporting Information). Since 1.7  $\mu$ g D-NG was applied to the SDS-PAGE, this corresponds on average to only 3 wt% HSA adsorbed to the nanocarriers.

Under the simplified assumption, that the nanocarriers would provide a perfectly hard and spherical surface ( $r = 50$  nm) and that HSA would yield a spherical size ( $r = 2.5$  nm), we roughly calculated that only 9% of D-NG's surface could theoretically be covered by the proteins (for detailed calculation see Figure S4, Supporting Information). Hence, this protein adsorption can hardly be considered as pronounced protein corona as only one twentieth of the surface of the nanocarrier would be covered.

To investigate whether plasma proteins beyond HSA, which could not be visualized by SDS PAGE, were found with our nanogel, a quantitative proteomic analysis was performed. In this analysis, the proteins of the samples were digested to tryptic peptides, which were then separated by liquid chromatography and analyzed by multi-stage mass spectrometry. Subsequently, the corresponding proteins were identified and label-free quantified by data processing and database search, as described recently.<sup>[12,27]</sup>

In analogy to previous proteomic analyses of nanocarriers using this method,<sup>[12,18]</sup> comparison of the AF4 fraction of the plasma incubated nanocarrier with the fractions of the plasma as well as the nanocarrier control were used to identify those proteins that got enriched by the presence of the nanogel. By this means, proteins which are simply co-eluting contaminants resulting from nanocarrier fabrication or co-eluting free plasma proteins could be excluded. As visualized by the Venn plot in Figure 4C, the overlap area of the nanocarrier and plasma controls states the number of the real enriched proteins in the plasma incubated D-NG sample. Thus, 65 proteins were identified and consequently co-eluting with D-NG after plasma incubation. The largest share of the total protein amounts accounts for HSA, with more than half of all detected proteins ( $\approx 52\%$ ) (Table S1, Supporting Information). This observation is completely different from the situation in block copolymer micelles,<sup>[12,18]</sup> for which only very small amounts of HSA were determined as co-eluting protein.

In our view, it seemed remarkable that so many different proteins were found on D-NG, even though we did not observe any size increase of the nanocarrier and an over-all very small loading with proteins. Furthermore, the previously reported profound stability of our nanocarrier in the blood stream makes opsonization by specific plasma proteins extremely unlikely. On this account, we wanted to investigate whether certain proteins were specifically enriched by strong binding to our nanocarrier or rather non-specifically diffused into the nano-sized hydrogel network and, therefore, passively accumulated. Thus, we also analyzed the applied pure plasma (not AF4 fractionated, from the identical plasma pool) using the same proteomic LC-MS method.

The relative abundance of the individual proteins in the plasma incubated nanogel was compared with their abundance in native plasma. This comparison revealed that most proteins could be attributed to a similar intensity (Figure 5A). Consequently, relative abundance of the most identified proteins is not enhanced through the presence of the nanocarrier.

Next, the abundance of the proteins in the pure plasma as well as the plasma incubated D-NG was normalized by dividing the intensity of the found proteins by the intensity of HSA, the most abundant plasma protein, in the respective sample. Thereby, we wanted to assess whether certain proteins that are hardly detectable compared to the large amount of HSA got indeed more

enriched or whether they were just found in the same amount relative to HSA in the original plasma. We compared the normalized relative intensity of the 65 enriched proteins (identified as shown in Figure 4C) with the relative intensity of these proteins in the pure plasma (Figure 5B). The results attested that the majority of proteins was indeed not enriched but partially found less. The same was confirmed by Figure 5C, in which the ratio (intensity of protein found in D-NG + plasma sample divided by intensity of protein) was plotted against their molecular weights. From 65 proteins only 14 revealed a ratio higher than 1, corresponding to a greater abundance. However, under common bioinformatical assumptions that a ratio over 2 (log 2 fold change  $> 1$ ) can be regarded as significant, no more than three proteins provided a considerable enrichment. These three proteins were identified as Transgelin-2, Serum amyloid P-component, and Pigment epithelium-derived factor (Table S2, Supporting Information). As far as we know, no opsonization is attributed to them and they are no typical protein corona components of other nanocarriers. The molecular weight of these three significantly enriched proteins is below 50 kDa, whereas relatively large proteins with molecular weights above 100 kDa seem to be excluded from the sponge-link structure of the nanogels. These proteins are thus rather depleted than accumulated relative to their abundance in plasma.

These results of the highly sensitive LC-MS proteomics analyses suggested that a passive, probably size-exclusive protein accumulation into our squaric ester-based nanogels occurred. It is expected that the proteins found in our plasma incubated D-NG sample rather randomly diffused into the nanocarrier's hydrophilic porous network and accumulated thereby passively. Except for three proteins with relatively small sizes that seem to penetrate best into the nanogel network, all other proteins are found in the same proportion or less to the same proteins in pure plasma, whereas larger proteins with sizes above 100 kDa cannot enter the hydrogel particle. In our opinion this behavior does not correspond to a defined protein particle affinity and thus, should not be described as distinct classical protein corona formation.

### 3. Conclusion

In this study, we investigated the blood plasma protein interaction of a highly "PEGylated" squaric ester-based nanogel system which already demonstrated profound stability in the blood stream after intravenous injections in previous studies.<sup>[8,10]</sup> Upon incubation in human blood plasma and subsequent separation by AF4, the nanocarrier maintained its size as shown by multi-angle DLS measurements. Furthermore, no signs of aggregate formation or size increase were evident from the AF4 elugrams. A slight intensity increase of the nanogel peak in those elugrams indicated a potential incorporation of proteins into the swollen nanogel network. However, as the nanocarrier's size was not affected, the absolute amount had to be very low. By means of the very sensitive silver staining of an SDS PAGE (detection limit in low ng-range), HSA, the most abundant plasma protein, could be visualized. The absolute amount of HSA was estimated as 3 wt% per nanocarrier. Since this amount barely corresponds to a full coverage of the nanocarrier's surface, we claim that our nanogels form by no means a pronounced classical protein corona.

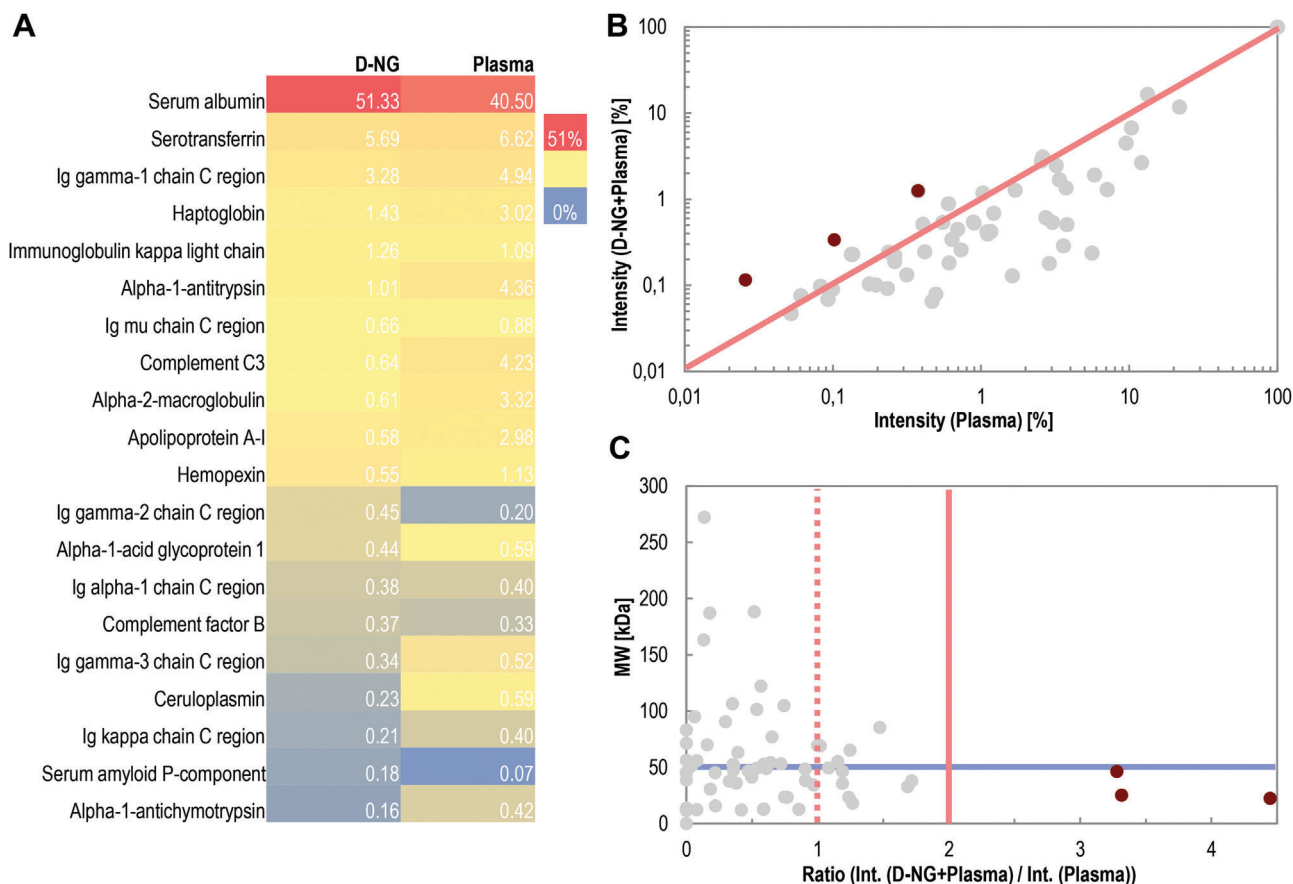


**Figure 5.** Comparative LC-MS analysis of plasma incubated D-NG AF4 fraction (D-NG + plasma) and pure native plasma. A) Heat map displaying the intensity of the 20 most abundant proteins in D-NG + plasma compared to their intensity in native plasma. B) Relative intensity of the identified 65 incorporated proteins detected in pure plasma against the relative intensity of these proteins detected in D-NG + plasma sample. C) Molecular weight of the 65 identified proteins against their intensity ratio (D-NG + plasma sample compared to pure plasma).

Interestingly, LC-MS analysis of the AF4 separated plasma incubated nanocarrier could identify 65 plasma proteins enriched in the particle fraction, for which HSA accounted for more than 50% relative abundance. Further proteomic LC-MS analysis of pure plasma revealed that the proportion of the proteins enriched in to the nanocarrier carrier was very similar to the proportion that these proteins naturally have in pure plasma. Since typically protein corona compositions significantly differ from the protein compositions of the physiological plasma,<sup>[28,29]</sup> we concluded that this kind of protein enrichment is engendered by the porous hydrogel morphology of our nanocarrier. Due to its high “PEGylation” not only on its shell, but also inside its core, it is a highly hydrophilic structure that would not interact with proteins inherently. The fully hydrated and swollen nanogel is held together by covalent crosslinks in the core forming a polymeric network that may be described as a sponge-like structure. Considering this morphology, we hypothesized that the identified proteins co-eluting by AF4 separation after plasma incubation are rather recorded because of their passive diffusion into the nanogel network (depending on their size) than chemical specific interactions/affinities of the proteins with the nanogel itself. We therefore suggest to further develop more sensitive separation strategies beyond the classical nanoparticle protein corona

isolation methods that will especially take into account the inner composition of nanogel particles (e.g., multiple consecutive AF4 injections could probably assist here, too).

From our recorded data, we expect that even though a variety of plasma proteins was identified, their low quantity might probably have only very little to no effect on the nanocarrier’s performance and stability in the blood stream. Their presence does not correspond to a classical particle surface protein corona but rather reflects even the highly inner stealth-like behavior of a porous hydrogel network.

## 4. Experimental Section

**Preparation of Nanogels:** The synthesis of ketal-crosslinked nanogels derived from the precursor polymer mPEG<sub>113</sub>-p(SQ-MA)<sub>38</sub> was described in detail earlier.<sup>[8]</sup> In analogy, after block copolymer self-assembly the micellar core was crosslinked using ketal-containing bisamine 2,2’-bis(aminoethoxy)propane, and hydrophilized using mPEG<sub>11</sub>-amine affording pH-degradable nanogels (D-NG).

**Dynamic Light Scattering after Human Plasma Incubation:** The stability of D-NG in human plasma was investigated by DLS both directly after plasma incubation as well as after subsequent AF4 separation. The human blood plasma used in this study was kindly provided from the

Transfusionszentrale of the University Medical Center of the Johannes Gutenberg-University Mainz. It was pooled of six healthy voluntary donors and stabilized with EDTA.

To analyze the size directly after plasma incubation, 50  $\mu\text{L}$  nanogel dispersion (10  $\text{mg mL}^{-1}$ ) was diluted with 1 mL plasma and incubated at 37  $^{\circ}\text{C}$  for 1 h. Subsequent DLS measurements were performed on a commercially available instrument, ALV/CGS-3 (ALV GmbH, Germany), consisting of an electronically controlled goniometer and an ALV-5004 multiple tau full-digital correlator (320 channels). A Uniphase He/Ne Laser (632.8 nm, 22 mW) was used as light source. For temperature-controlled measurements the instrument was equipped with a thermostat from Julabo. The angular dependent measurements were performed between 30 $^{\circ}$  and 150 $^{\circ}$  in 20 $^{\circ}$  steps. Data analysis was performed according to the procedure described by Rausch et al.<sup>[22]</sup>

For DLS experiments after plasma incubation and subsequent AF4 separation the collected nanogel fractions from the AF4 were used. Prior to each measurement, dust was removed by filtration through GHP syringe filters (0.2  $\mu\text{m}$  pore size, Acrodisc) in a dust-free flow box. Measurements were performed in dust-free cylindrical cells (20 mm diameter, Suprasil, Heraeus, Hanau, Germany)

**Asymmetrical Flow-Field Flow Fractionation:** Prior to AF4 separation, D-NG (10  $\text{mg mL}^{-1}$ ) were incubated with EDTA-stabilized human blood plasma (v:v, 3:1) at 37  $^{\circ}\text{C}$  for 1 h. Since sufficient AF4 separations were restricted to a maximum plasma concentration of 5 vol%, the incubation sample was diluted after incubation time with PBS to a nanogel concentration of 1.5  $\text{mg mL}^{-1}$  and 5 vol% plasma.

AF4 measurements were performed using a commercial system (ConSenxuS GmbH, Ober-Hilbersheim, Germany). The set up comprised a constaMETRICR 3200 main pump and a Spectra Series UV150 detector (both Thermo Separation), a Dark V3 LS Detector (ConSenxuS GmbH), a P-3500 injection pump (Pharmacia), a LV-F flow controller (HORIBA STEC, Kyoto, Japan), an In-Line Degasser-AF (Waters, Milford, Ma, US), and a separation channel with a 190  $\mu\text{m}$  spacer and a membrane (regenerated cellulose, molecular weight cut-off (MWCO) 10 kDa), which was suitable for protein separation.

For the measurements PBS containing 200 mM sodium azide was used as solvent. The main flow was 1.75  $\text{mL min}^{-1}$ , while the crossflow of the measurements was set to 0.75  $\text{mL min}^{-1}$ . The measurements were carried out in triplicate originating from three separate incubation experiments. Nanogel fractions were collected from 10 to 16.67 min (600 to 1000 s). The collected fractions were concentrated using spin filtration (Amicon Ultra Centrifugal Filters, regenerated cellulose, MWCO 3 kDa).

**LC-MS Sample Preparation:** Prior to LC-MS measurements, a tryptic protein digestion was performed according to the "Single-Pot Solid-Phase-Enhanced Sample Preparation" (SP3) protocol.<sup>[27]</sup> The exact procedure was recently described by Alberg et al. and performed analogously.<sup>[12]</sup>

**LC-MS Analysis and Data Processing:** Liquid chromatography (LC) of tryptic peptides was performed on an Ultimate 3000 nanoUPLC (Thermo Scientific) equipped with a reversed phase C18 column (HSS-T3 C18 1.8  $\mu\text{m}$ , 75  $\mu\text{m}$   $\times$  250 mm, Waters Corporation). Mobile phase A was 0.1% v/v formic acid (FA) and 3% v/v dimethyl sulfoxide (DMSO) in water. Mobile phase B was 0.1% v/v FA and 3% v/v DMSO in acetonitrile (ACN). Peptides were separated with 300  $\text{nL min}^{-1}$  at 55  $^{\circ}\text{C}$  using a 60 min linear gradient. MS analysis of eluting peptides was performed using an Orbitrap Exploris 480 (Thermo Scientific) by data-dependent acquisition (DDA). Full scan MS1 spectra were collected over a range of 350–1600  $m/z$  with a mass resolution of 60 000 @ 200  $m/z$  using an automatic gain control (AGC) target of 300%, maximum injection time was set to "Auto" and RF lens to 40%. The TOP10 intensity signals within an isolation window of 1.4 Da above a signal threshold of  $2 \times 10^4$  and a charge of 2–6 were selected as precursors for fragmentation using higher energy collisional dissociation (HCD) with normalized collision energy of 30. The resulting fragment ion  $m/z$  ratios were measured as MS2 spectra over an automatically selected  $m/z$  range with a mass resolution of 15 000 @ 200  $m/z$ , AGC target was set to "Standard" and maximum injection time to "Auto".

Raw MS data processing and database search was performed using MaxQuant v.2.0 with integrated search engine Andromeda. The resulting proteins were searched against UniProt Human proteome database

(UniProtKB release 2018\_09, 16 991 entries) supplemented with a list of common contaminants. The database search was specified by trypsin as enzyme for digestion and peptides with up to two missed cleavages were included. Furthermore, Carbamidomethyl cysteine was set as fixed modification and oxidized methionine as variable modification. False discovery rate (FDR) assessment for peptide and protein identification was done using the target-decoy strategy by searching a reverse database and was set to 0.01 for database search in MaxQuant.

By using TOP3 quantification,<sup>[30]</sup> absolute in-sample amounts of proteins were calculated. Statistical analysis was done by performing two-tailed, paired -tests and subsequent Benjamini–Hochberg correction.<sup>[31]</sup> Q-values < 0.05 were considered as significant. To be enriched in a considerable amount in a given condition the log2 ratio threshold needed to be  $\geq 1$ .

**SDS Page:** SDS PAGE analyses were performed using polyacrylamide gels composed of 12% separation gel and 5% stacking gel using a Mini-PROTEAN Tetra Vertical Electrophoresis Cell (BIO-RAD, Hercules, CA, USA). Gel electrophoresis was performed for 45 min at 200 V.

For sample preparation 7.5  $\mu\text{L}$  of each sample was incubated with 2.5  $\mu\text{L}$  NuPAGE LDS Sample Buffer (Invitrogen, Waltham, MA, USA) and heated up for 5 min at 95  $^{\circ}\text{C}$ . For molecular weight comparison Novex Sharp Pre-Stained Protein Standard (Invitrogen) was used. Proteins were stained using silver or Coomassie blue staining.

**Additional Information:** Parts of schematic illustrations in TOC, Figures 2, 3A, and 4A were created with BioRender.com.

## Supporting Information

Supporting Information is available from the Wiley Online Library or from the author.

## Acknowledgements

A.H. and L.N. acknowledges support by the Max Planck Graduate Center with the Johannes Gutenberg-University Mainz (MPGC). Moreover, L.N. kindly acknowledges financial support by the DFG through the Emmy Noether program. In addition, L.N., R.Z., S.T., and K.L. thank the DFG for funding of the collaborative research center SFB 1066. Both A.H. and L.N. would further like to thank Tanja Weil for providing access to excellent laboratory facilities.

Open Access funding enabled and organized by Projekt DEAL.

## Conflict of Interest

The authors declare no conflict of interest.

## Author Contributions

A.H. performed nanogel fabrication, and SDS PAGE analysis; I.A. conducted AF4 measurements; C.L. performed LC-MS measurements and data processing; C.R. conducted light scattering measurements; S. M., K. L., S.T., and R.Z. contributed analytical tools; A.H., R.Z., and L.N. analyzed data; L. N. supervised the project, A.H. and L.N. wrote the paper.

## Data Availability Statement

The data that support the findings of this study are available in the supporting information of this article.

## Keywords

drug delivery, nanogels, PEGylation, protein corona, stealth

Received: April 1, 2022  
Revised: May 17, 2022  
Published online: June 24, 2022

- [1] A. C. Anselmo, S. Mitragotri, *Bioeng. Transl. Med.* **2016**, *1*, 10.
- [2] D. Docter, D. Westmeier, M. Markiewicz, S. Stolte, S. K. Knauer, R. H. Stauber, *Chem. Soc. Rev.* **2015**, *44*, 6094.
- [3] S. Tenzer, D. Docter, J. Kuharev, A. Musyanovych, V. Fetz, R. Hecht, F. Schlenk, D. Fischer, K. Kiouptsi, C. Reinhardt, K. Landfester, H. Schild, M. Maskos, S. K. Knauer, R. H. Stauber, R. H. Stauber, *Nat. Nanotechnol.* **2013**, *8*, 772.
- [4] T. Cedervall, I. Lynch, S. Lindman, T. Berggård, E. Thulin, H. Nilsson, K. A. Dawson, S. Linse, S. Linse, *Proc. Natl. Acad. Sci. U. S. A.* **2007**, *104*, 2050.
- [5] N. Bertrand, P. Grenier, M. Mahmoudi, E. M. Lima, E. A. Appel, F. Dormont, J.-M. Lim, R. Karnik, R. Langer, O. C. Farokhzad, O. C. Farokhzad, *Nat. Commun.* **2017**, *8*, 777.
- [6] S. Schöttler, K. Landfester, V. Mailänder, *Angew. Chem. Int. Ed.* **2016**, *55*, 8806.
- [7] W. Richtering, I. Alberg, R. Zentel, *Small* **2020**, *16*, 2002162.
- [8] A. Huppertsberg, L. Kaps, Z. Zhong, S. Schmitt, J. Stickdorn, K. Deswarte, F. Combes, C. Czysch, J. De Vrieze, S. Kasmi, N. Choteschovsky, A. Klefenz, C. Medina-Montano, P. Winterwerber, C. Chen, M. Bros, S. Lienenklaus, N. N. Sanders, K. Koynov, D. Schuppan, B. N. Lambrecht, S. A. David, B. G. De Geest, L. Nuhn, *J. Am. Chem. Soc.* **2021**, *143*, 9872.
- [9] L. Kaps, A. Huppertsberg, N. Choteschovsky, A. Klefenz, F. Durak, B. Schrörs, M. Diken, E. Eichler, S. Rosigkeit, S. Schmitt, C. Leps, A. Schulze, F. Foerster, E. Bockamp, B. G. De Geest, K. Koynov, H.-J. Räder, S. Tenzer, F. Marini, D. Schuppan, L. Nuhn, K. P. H.-D. Wooley, *Proc. Natl. Acad. Sci. U. S. A.* **2022**, *119*, e2122310119.
- [10] S. Schmitt, A. Huppertsberg, A. Klefenz, L. Kaps, V. Mailänder, D. Schuppan, H.-J. Butt, L. Nuhn, K. Koynov, *Biomacromolecules* **2022**, *23*, 1065.
- [11] S. Tenzer, D. Docter, S. Rosfa, A. Włodarski, J. Kuharev, A. Reikik, S. K. Knauer, C. Bantz, T. Nawroth, C. Bier, J. Sirirattanapan, W. Mann, L. Treuel, R. Zellner, M. Maskos, H. Schild, R. H. Stauber, *ACS Nano* **2011**, *5*, 7155.
- [12] I. Alberg, S. Kramer, M. Schinnerer, Q. Hu, C. Seidl, C. Leps, N. Drude, D. Möckel, C. Rijcken, T. Lammers, M. Diken, M. Maskos, S. Morsbach, K. Landfester, S. Tenzer, M. Barz, R. Zentel, *Small* **2020**, *16*, 1907574.
- [13] W. Fraunhofer, G. Winter, G. Winter, *Eur. J. Pharm. Biopharm.* **2004**, *58*, 369.
- [14] C. Weber, J. Simon, V. Mailänder, S. Morsbach, K. Landfester, *Acta Biomater.* **2018**, *76*, 217.
- [15] T. Mićlausz, C. Beer, J. Chevallier, C. Scavenius, V. E. Bochenkov, J. J. Enghild, D. S. Sutherland, *Nat. Commun.* **2016**, *7*, 11770.
- [16] J. Wang, U. B. Jensen, G. V. Jensen, S. Shipovskov, V. S. Balakrishnan, D. Otzen, J. S. Pedersen, F. Besenbacher, D. S. Sutherland, D. S. Sutherland, *Nano Lett.* **2011**, *11*, 4985.
- [17] S. Winzen, S. Schoettler, G. Baier, C. Rosenauer, V. Mailänder, K. Landfester, K. Mohr, *Nanoscale* **2015**, *7*, 2992.
- [18] I. Alberg, S. Kramer, C. Leps, S. Tenzer, R. Zentel, I. Alberg, S. Kramer, R. Zentel, C. Leps, S. Tenzer, *Macromol. Biosci.* **2021**, *21*, 2000414.
- [19] E. Ostuni, R. G. Chapman, R. E. Holmlin, S. Takayama, G. M. Whitesides, *Langmuir* **2001**, *17*, 5605.
- [20] M. G. Vence, M. D. P. Chantada-Vázquez, S. Vázquez-Estévez, J. M. Gamalesse-Teijeiro, S. B. Bravo, C. Núñez, *Clin. Chim. Acta* **2020**, *501*, 102.
- [21] M. Hadjidemetriou, Z. Al-Ahmady, M. Buggio, J. Swift, K. Kostarelos, *Biomaterials* **2019**, *188*, 118.
- [22] K. Rausch, A. Reuter, K. Fischer, M. Schmidt, *Biomacromolecules* **2010**, *11*, 2836.
- [23] C. Weber, M. Voigt, J. Simon, A.-K. Danner, H. Frey, V. Mailänder, M. Helm, S. Morsbach, K. Landfester, *Biomacromolecules* **2019**, *20*, 2989.
- [24] C. Weber, J. Simon, V. Mailänder, S. Morsbach, K. Landfester, *Acta Biomater.* **2018**, *76*, 217.
- [25] M. Chevallet, S. Luche, T. Rabilloud, T. Rabilloud, *Nat. Protoc.* **2006**, *1*, 1852.
- [26] J. L. Brunelle, R. C. Green, *Methods Enzymol.* **2014**, *541*, 161.
- [27] M. Sietlaff, J. Kuharev, T. Bohn, J. Hahlbrock, T. Bopp, S. Tenzer, U. Distler, *J. Proteome Res.* **2017**, *16*, 4060.
- [28] M. P. Monopoli, C. Åberg, A. Salvati, K. A. Dawson, *Nat. Nanotechnol.* **2012**, *7*, 779.
- [29] C. D. Walkey, W. C. W. Chan, *Chem. Soc. Rev.* **2012**, *41*, 2780.
- [30] P. Navarro, J. Kuharev, L. C. Gillet, O. M. Bernhardt, B. MacLean, H. L. Röst, S. A. Tate, C. C. Tsou, L. Reiter, U. Distler, G. Rosenberger, Y. Perez-Riverol, A. I. Nesvizhskii, R. Aebersold, *Nat. Biotechnol.* **2016**, *34*, 1130.
- [31] Y. Benjamini, Y. Hochberg, *J. R. Stat. Soc. B* **1995**, *57*, 289.